Journal of Power Sources 195 (2010) 8336–8340

Contents lists available at ScienceDirect

Journal of Power Sources

journal homepage: www.elsevier.com/locate/jpowsour

Short communication

High-capacity organic positive-electrode material based on a benzoquinone derivative for use in rechargeable lithium batteries

Masaru Yao*, Hiroshi Senoh, Shin-ichi Yamazaki, Zyun Siroma, Tetsuo Sakai, Kazuaki Yasuda

Research Institute for Ubiquitous Energy Devices, National Institute of Advanced Industrial Science and Technology (AIST), 1-8-31 Midorigaoka, Ikeda, Osaka 563-8577, Japan

ARTICLE INFO

Article history:
Received 26 May 2010
Accepted 21 June 2010
Available online 25 June 2010

Keywords:
Organic cathode material
Lithium ion battery
High capacity
Multi-electron redox
DFT calculation

ABSTRACT

The performance of 2,5-dimethoxy-1,4-benzoquinone (DMBQ) as an active material for rechargeable lithium batteries was investigated. A positive-electrode that incorporated DMBQ showed an initial discharge capacity of 312 mAh g^{-1} with an average voltage of 2.6 V vs. Li^+/Li. This discharge capacity corresponds to a benzoquinone-based two-electron redox behavior, and is more than twice that of the conventional positive-electrode material lithium cobalt oxide ($LiCoO_2$). Furthermore, the positive-electrode with DMBQ showed fair cycle-life performance. Theoretical quantum calculations based on the density functional theory (DFT) were also performed to clarify the mechanism of the electrochemical properties of the solid state of DMBQ.

© 2010 Elsevier B.V. All rights reserved.

1. Introduction

Throughout the more than 150-year history of rechargeable batteries, progress has continued, and these batteries are now widely used as power sources in everyday electronic devices. Moreover, the demand for batteries has recently been increasing due to concerns about global environmental issues. Among various rechargeable batteries, lithium-based batteries have been widely studied because of their high energy characteristics, and various materials have been proposed to improve their performance. In addition, low-polluting materials are becoming more desirable due to considerations of environmental effects, and organic materials that do not include any heavy metals have recently been attracting attention as alternative active materials [1,2].

Many organic positive-electrode materials have been proposed so far. They can be classified into several categories, each of which offers drawbacks and advantages. The first category includes classical conductive polymers, represented by polyaniline or polythiophene, which have a practical capacity of about 150 mAh g^{-1} [3]. The capacities in this category cannot become large because of the upper limit of the doping level [3]. The second category is a series of organosulfur compounds bearing disulfide bonds, and these are expected to show high discharge capacities of up to about 500 mAh g^{-1}. However, their cycle-life performance is inadequate because of the dissolution of the active materials into the electrolytes [4,5]. Pendant-type polymers based on a tetramethylpiperidine-*N*-oxyl (TEMPO) [6] or ferrocene [7] skeleton have been studied as a third type of active material, and these have practical capacities of about 100 mAh g^{-1}. Recently, low-molecular-weight lithiated oxocarbon salts, which show high capacities up to about 500 mAh g^{-1} and fair cycle stabilities, have been reported; however, these materials still show limited variation [8,9].

Quinone-based materials have been studied as another type of organic active material since the 1980s, since the quinone skeleton shows a two-electron redox reaction [10–12]. The quinone skeleton is frequently found in biological molecules, such as vitamin K, coenzyme Q_{10} (ubiquinone) and plastoquinone [13–15], and some quinone derivatives play important roles as redox materials in biological electron-transport systems [15]. If we could use a redox system that includes 1,4-benzoquinone, which is the simplest quinine derivative, as a positive-electrode material, a large capacity of up to about 500 mAh g^{-1} should be expected, although the use of 1,4-benzoquinone itself is practically difficult because of its high capacity for sublimation. Several pioneering works have tried to apply this redox reaction to battery systems through the synthesis of various polymers [3,10–12]. However, the two-electron redox reaction in battery materials has not been realized in most cases due to various problems, such as the dissolution of these organic compounds into the electrolytes, the instability of intermediate radical species, and low electrical conductivity.

As a novel benzoquinone-based active material, we focused our attention on 2,5-dimethoxy-1,4-benzoquinone (DMBQ) (Fig. 1). In the crystal state, each molecule is strongly connected to its neighboring molecules by π–π interaction as well as weak hydrogen bonding [16,17]. Due to these intermolecular forces, the solubility

* Corresponding author. Tel.: +81 72 751 9653; fax: +81 72 751 9629.
E-mail address: m.yao@aist.go.jp (M. Yao).

0378-7753/$ – see front matter © 2010 Elsevier B.V. All rights reserved.
doi:10.1016/j.jpowsour.2010.06.069

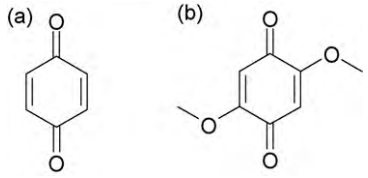

Fig. 1. Chemical structures of (a) 1,4-benzoquinone and (b) 2,5-dimethoxy-1,4-benzoquinone (DMBQ).

of DMBQ in solvents is decreased. Specifically, the solubility values of DMBQ in acetone, ethyl acetate, and tetrahydrofuran at 20 °C are 0.1, 0.04, and 0.02 mg cm^{-3}, respectively. The peripheral methoxy groups can act as protective groups for the radical intermediate that is formed during the redox process. In the present study, we discovered that DMBQ shows high discharge capacity and fair cycle stability. This paper presents the preliminary electrochemical properties, including battery performance.

2. Experimental

2,5-Dimethoxyl-1,4-benzoquinone (DMBQ) was purchased from Tokyo Kasei Corp. and used without further purification. The specific gravity calculated from crystallographic data of this compound is 1.50 [16].

Cyclic voltammetry (CV) was applied to a saturated solution of DMBQ in an acetonitrile/tetra-*n*-butylammonium perchlorate system (0.1 mol L^{-1}) with a Ag^+/Ag reference electrode using an electrochemical analyzer (SI 1280B, Solartron) to estimate the properties of DMBQ as an active material. The voltammogram was recorded at a scan speed of 50 mV s^{-1} with a potential range of −0.5 to −2.5 V vs. Ag^+/Ag at room temperature.

A coin-type sealed cell for the battery test was prepared as follows. A positive-electrode composite sheet was first prepared by mixing a powder of DMBQ, acetylene black as a conductive additive, and polytetrafluoroethylene as a binder in a weight ratio of 4:5:1 using a mortar. The sheet was then attached to an aluminum mesh, and the resultant positive-electrode was dried. The amount of active material deposited was approximately 3 mg cm^{-2}. The prepared positive-electrode and a lithium metal negative-electrode were placed in an R2032 coin-type cell case with a glass filter as a separator. After an electrolyte of γ-butyl lactone containing lithium perchlorate (1.0 mol L^{-1}) was added, the cell case was sealed.

In the charge/discharge cycle-life test, the prepared coin-type cell was galvanostatically discharged at a current density with a cutoff voltage of 2.0 V vs. Li^+/Li, and galvanostatically charged with a cutoff voltage of 3.4 V vs. Li^+/Li followed by potentiostatic charge at that voltage. The charge/discharge tests were performed with computer-controlled systems (BLS series, Keisokuki Center Co. Ltd.) (ABE system, Electrofield Co. Ltd.) equipped with a thermostatic chamber.

Ex situ X-ray diffraction (XRD) measurement was used to analyze the change in the crystal structure of DMBQ upon charge/discharge cycling using a diffractometer (X′Pert PRO MPD, PANalytical B.V.).

DFT calculations were performed using the GAUSSIAN 03 program package [18] to obtain theoretical insight into the stability of a radical compound obtained during the charge/discharge process and the electronic structure of the crystal state of DMBQ. A popular B3LYP hybrid functional [19,20] with the disuse function that included a split valence basis set of 6-31+G(d) was used. For calculation of the monomer state, the geometry was optimized. For estimation of the electronic structure of the crystal state, a single point calculation was performed at the same level on clusters composed of 20 monomer units using the coordinates extracted from the X-ray analysis [16]. The calculated molecular orbitals were visualized by Gauss View 3.0 [21]

3. Results and discussion

To evaluate the preliminary battery performance of DMBQ, cyclic voltammetry was first carried out. Fig. 2a shows the cyclic voltammogram of DMBQ. As shown, DMBQ showed quasi-reversible stepwise redox behavior, in which two redox pairs were observed at around −1.0 and −1.6 V vs. Ag^+/Ag, with peak separations of 0.07 and 0.08 V, respectively. The recorded potentials can

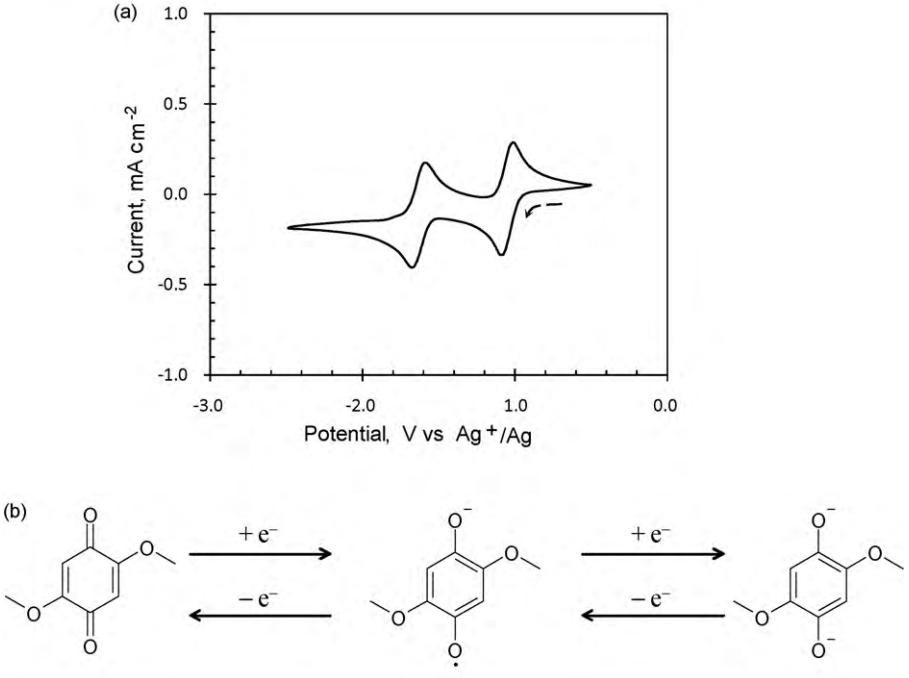

Fig. 2. (a) Cyclic voltammogram of an acetonitrile solution of DMBQ (scan rate: 50 mV s^{-1}). (b) Schematic drawing of the redox mechanism of DMBQ.

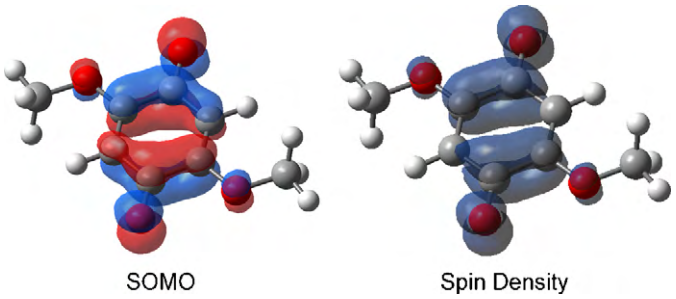

Fig. 3. Optimized structures of the anion radical state of DMBQ, its SOMO, and spin density distribution. Computation was performed at the unrestricted B3LYP/6-31+G(d) level with a polarizable continuum model to reflect polar solvent effects. Oxygen, carbon, and hydrogen atoms are shown in red, gray, and white, respectively. (For interpretation of the references to color in this figure legend, the reader is referred to the web version of the article.)

be converted to the approximate positions at 2.8 and 2.2 V vs. Li^+/Li. The pair at a higher potential reflects the redox reaction between the neutral state of DMBQ and the monoanion radical species and that at a lower potential is ascribed to the redox reaction between the monoanion radical and the dianion species, as shown schematically in Fig. 2b.

In some cases, radical species can rapidly decompose through disproportionation, dimerization, reaction with solvent molecules, and so on; however, the observed voltammogram also implies that the anion radical species is highly stable. To obtain theoretical insight into the stability of the radical intermediate obtained during the redox process, a theoretical quantum calculation based on the density functional theory (DFT) was performed. Fig. 3 shows the optimized structure of the anion radical state of DMBQ, the shape of the singly occupied molecular orbital (SOMO), and the spin density distribution. The SOMO of the anion radical state of DMBQ is delocalized over the benzoquinone skeleton due to aromaticity, and the spin density is widely distributed over the molecules, which can stabilize the radical state of this molecule [22,23]. In addition, the methoxy groups at the 2,5-positions can act as protecting groups. This characteristic spin distribution and the substituent steric effect are considered to synergistically stabilize the anion radical species during the redox process. These results imply that DMBQ may be suitable for use as a positive-electrode active material.

The battery performance of DMBQ was evaluated by preparing a coin-type sealed cell. Fig. 4a shows the initial discharge and subsequent charge curves of the positive-electrode prepared using DMBQ. A characteristic discharge curve consisting of two plateau voltage regions at around 2.8 and 2.5 V vs. Li^+/Li was observed. The first plateau observed at a higher potential reflects the reduction of DMBQ itself to a monoanion radical species, and the second plateau at a lower potential is ascribed to the additional reduction of the monoanion radical species to the dianion species, as discussed in the section on the CV measurement (Fig. 2b). To our surprise, the observed discharge capacity of 312 mAh g^{-1} is extremely close to the theoretical value of 319 mAh g^{-1}, which assumes the full two-electron-transfer reaction of DMBQ, and this value is more than twice the practical capacity of conventional $LiCoO_2$ (~140 mAh g^{-1}). Furthermore, to the best of our knowledge, this value is the largest among various benzoquinone derivatives reported elsewhere [10–12]. The average voltage of 2.6 V vs. Li^+/Li for this compound is lower than the average voltage of 3.8 V vs. Li^+/Li for $LiCoO_2$, however, the weight energy density of DMBQ is still 1.5 times greater than that of $LiCoO_2$.

A conventional cycle-life test was also carried out for the prepared positive-electrode, as shown in Fig. 4b. Although the capacity decreased slightly upon cycling, it was still 255 mAh g^{-1} after 10 cycles. There have been a few reports on the battery performance

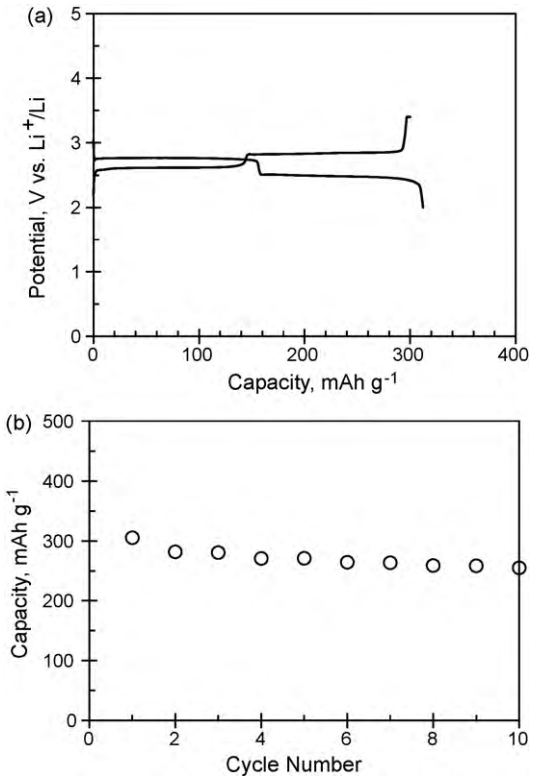

Fig. 4. (a) Initial discharge and charge curves of the positive-electrode using DMBQ (current density: 10 mA g^{-1}, temperature: 30 °C). (b) Cycle-life performance of the electrode using DMBQ (current density: 20 mA g^{-1}, potential range: 2.0–3.4 V vs. Li^+/Li, temperature: 30 °C).

of such low-molecular-weight compounds [24,25], and their discharge capacities often decrease drastically upon cycling. One of the reasons for this decrease in capacity is the dissolution of redox active molecules into the electrolyte. In our case, the cycle-life performance of DMBQ is relatively good compared to those of organic active materials based on low-molecular-weight compounds.

To evaluate the change in the crystal structure of DMBQ upon cycling, an XRD measurement was performed on the electrodes after several cycles. Fig. 5 shows a comparison of the XRD patterns of the charged states of the electrode upon cycling along with that of the powder of DMBQ itself. With the first discharge, the XRD pattern

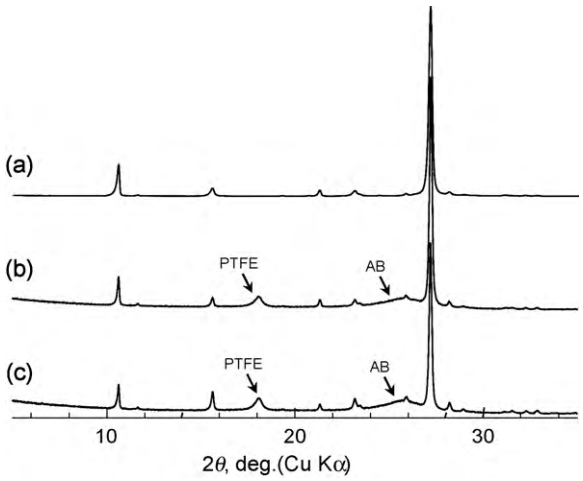

Fig. 5. XRD patterns of (a) DMBQ powder, (b) the electrode after one cycle, and (c) the electrode two cycles. All patterns reflect the oxidized (charged) states.

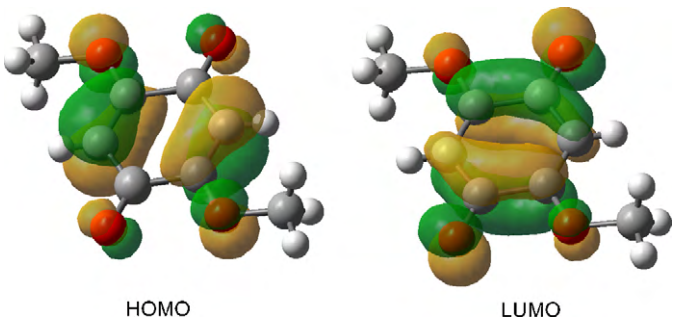

Fig. 6. Optimized structure of the monomer state of DMBQ and the calculated HOMO and LUMO. Computation was performed at the unrestricted B3LYP/6-31+G(d) level. Oxygen, carbon, and hydrogen atoms are shown in red, gray, and white, respectively. (For interpretation of the references to color in this figure legend, the reader is referred to the web version of the article.)

changed and became broad; this pattern was reversed by subsequent charging. Furthermore, each XRD pattern did not change at least during a few cycles. This observation indicates that the change in the crystal structure of this compound via redox is reversible. As described above, this compound shows low solubility in common organic solvents including organic electrolyte solution. In addition, the high reversibility of the bulk structure upon cycling is considered to contribute to the observed fair cycle-life performance.

Furthermore, a DFT calculation was performed to obtain theoretical insight into the electronic conduction mechanism of the crystalline state of DMBQ during the charge/discharge process, since a high capacity up to the theoretical value cannot be expected without some electron-transfer pathways that connect each molecule of DMBQ in the crystal. First, the calculated highest occupied molecular orbital (HOMO) and lowest unoccupied molecular orbital (LUMO) of the monomer state of DMBQ are shown in Fig. 6. Each molecular orbital has π bond characteristics and is delocalized over the whole π-system of the molecule. The electronic state of the crystalline state of DMBQ was estimated using cluster models composed of 20 molecular units; the coordinates extracted from X-ray analysis data [16] were used for this calculation. In the crystal, the molecules of DMBQ are aligned one-dimensionally for some directions, as shown in Fig. 7a. Each molecule is stacked in the d-1 direction by π–π interaction, and is aligned horizontally for the d-2 and d-3 directions by hydrogen bonding [17]. The calculated energy levels of the clusters are shown in Fig. 7b along with that of the monomer. For the cluster along the d-1 direction, the energy levels that originated from HOMO and LUMO are both expanded due to the overlap of their π-orbitals, and form an electronic band structure. On the other hand, the widths of the energy levels for the clusters along the d-2 and d-3 directions are narrower, which indicates less overlapping of orbitals for these directions. Therefore, the electronic band structure along the π-stacked direction appears to be the main electron-transfer pathway during the charge/discharge process. Due to this one-dimensionally stacked structure and the resulting electronic band structure, electrons can flow into the interior of the crystal of DMBQ, which is not directly attached to the current collector or a conductive additive. While the mechanism of electronic conduction or ionic conduction in the crystal of DMBQ has not been experimentally revealed at present, the calculated characteristic electronic structure should contribute to the high availability of the molecules of DMBQ in the crystal during the charge/discharge process.

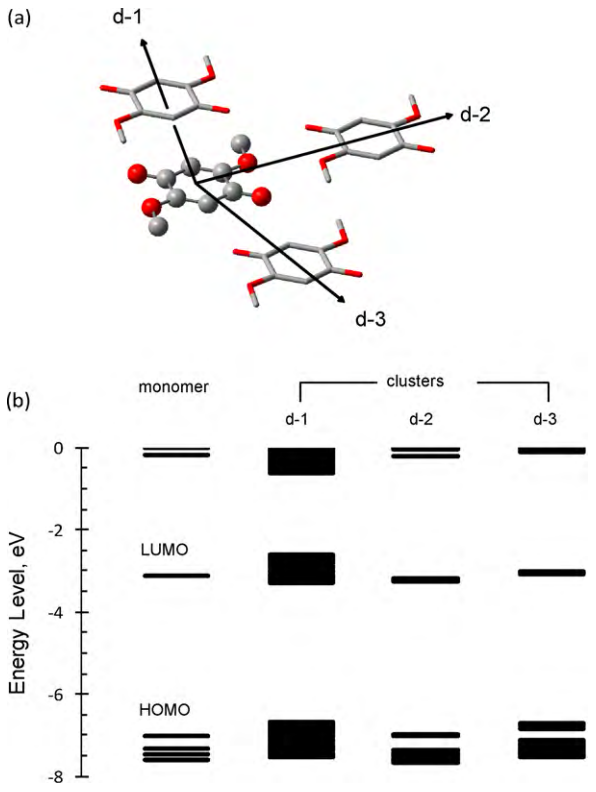

Fig. 7. (a) One-dimensionally aligned DMBQ in the crystal. d-1, d-2, and d-3 represent the directions of cluster coordinates. Hydrogen atoms are omitted for clarity. (b) Calculated energy diagrams of the monomer and clusters of DMBQ. Computation was performed at the restricted B3LYP/6-31+G(d) level.

4. Conclusions

The performance of 2,5-dimethoxy-1,4-benzoquinone (DMBQ) was investigated as an active material for use in rechargeable lithium batteries. A positive-electrode that was prepared using DMBQ showed stepwise two-electron redox behavior, and gave an initial discharge capacity of 312 mAh g^{-1} with an average voltage of 2.6 V vs. Li^+/Li. In addition, the positive-electrode exhibited fair cycle-life performance: more than 250 mAh g^{-1} even after 10 cycles. The low solubility of DMBQ due to π–π interaction and hydrogen bonding was considered to suppress the dissolution of the active material into the electrolyte during the charge/discharge process. Furthermore, the formation of an electronic band structure along one-dimensionally stacked DMBQ was suggested by a quantum calculation, and this can act as an electron-transfer pathway during charge/discharge.

The electrochemical properties of 1,4-benzoquinone derivatives can be adjusted by some chemical modifications. Further improvements in battery voltage, capacity, and cycle-life performance may be realized by optimizing the chemical structure and the cell composition.

Acknowledgement

The authors thank Ms. M. Araki at the National Institute of Advanced Industrial Science and Technology for her assistance with the experiments.

References

[1] H. Nishide, K. Oyaizu, Science 319 (2008) 737–738.
[2] M. Armand, J.-M. Tarascon, Nature 451 (2008) 652–657.
[3] P. Novák, K. Müller, K.S.V. Santhanam, O. Hass, Chem. Rev. 97 (1997) 207–281.
[4] M. Liu, S.J. Visco, L.C. De Jonghe, J. Electrochem. Soc. 138 (1991) 1891–1895.
[5] N. Oyama, T. Tatsuma, T. Sato, T. Sotomura, Nature 373 (1995) 598–600.
[6] K. Nakahara, S. Iwasa, M. Satoh, Y. Morioka, M. Suguro, E. Hasegawa, Chem. Phys. Lett. 359 (2002) 351–354.
[7] K. Tamura, N. Akutagawa, M. Satoh, J. Wada, T. Masuda, Macromol. Rapid Commun. 29 (2008) 1944–1949.

[8] H. Chen, M. Armand, G. Demailly, F. Dolhem, P. Poizot, J.-M. Tarascon, ChemSusChem 1 (2008) 348–355.
[9] H. Chen, M. Armand, M. Courty, M. Jiang, C.P. Grey, F. Dolhem, J.-M. Tarascon, P. Poizot, J. Am. Chem. Soc. 131 (2009) 8984–8988.
[10] J.S. Foos, S.M. Erker, L.M. Rembetsy, J. Electrochem. Soc. 133 (1986) 836–841.
[11] T.L. Gall, H.R. Reiman, M. Grossel, J.R. Owen, J. Power Sources 119–121 (2003) 316–320.
[12] J.F. Xiang, C.X. Chang, M. Li, S.M. Wu, L.J. Yuan, J.T. Sun, Cryst. Growth Des. 8 (2008) 280–282.
[13] P.A. Loach, Handbook of Biochemistry and Molecular Biology, in: G.D. Fasman (Ed.), Physical and Chemical Data, Vol. I, 3rd ed., CRC Press, 1976, pp. 123–130.
[14] R.C. Prince, P.L. Dutton, J.M. Bruce, FEBS Lett. 160 (1983) 273–276.
[15] J.M. Berg, J.L. Tymoczko, L. Stryer, Biochemistry, 5th ed., W.H. Freeman and Company, New York, 2002 (For example).
[16] H. Bock, S. Nick, W. Seitz, C. Nather, J.W. Bats, Z. Naturforsch. Teil B Chem. Sci. 51 (1996) 153–171.
[17] E.M.D. Keegstra, V. van der Mieden, J.W. Zwikker, L.W. Jenneskens, A. Schouten, H. Kooijman, N. Veldman, A.L. Spek, Chem. Mater. 8 (1996) 1092–1105.
[18] Gaussian 03, Revision E.01, M.J. Frisch et al., Gaussian, Inc., Wallingford, CT, 2004.
[19] A.D. Becke, Phys. Rev. A38 (1988) 3098–3100.
[20] C. Lee, W. Yang, R.G. Parr, Phys. Rev. B37 (1988) 785–789.
[21] GaaussView, Version 4.1.2, Roy Dennington II, K. Todd, J. Millam, K. Eppinnett, W.L. Hovell, G. Ray, Semichem, Inc., Shawnee Mission, KS, 2003.
[22] M. Yao, H. Inoue, N. Yoshioka, Chem. Phys. Lett. 402 (2005) 11–16.
[23] M. Yao, S. Asakura, M. Abe, H. Inoue, N. Yoshioka, Cryst. Growth Des. 5 (2005) 413–417.
[24] X. Han, C. Chang, L. Yuan, T. Sun, J. Sun, Adv. Mater. 19 (2007) 1616–1621.
[25] Z. Song, H. Zhan, Y. Zhou, Chem. Commun. 4 (2009) 448–450.